Advances in Radiation Oncology (2022) 7, 100854

advances in radiation oncology

www.advancesradonc.org

Scientific Article

Dynamic Contrast-enhanced and Diffusion-weighted Magnetic Resonance Imaging for Response Evaluation After Single-Dose Ablative Neoadjuvant Partial Breast Irradiation

Jeanine E. Vasmel, MD,[a,1,*] Maureen L. Groot Koerkamp, MSc,[a,1] Stefano Mandija, PhD,[a,b] Wouter B. Veldhuis, PhD,[c] Maaike R. Moman, PhD,[c] Martijn Froeling, PhD,[c] Bas H.M. van der Velden, PhD,[d] Ramona K. Charaghvandi, PhD,[e] Celien P.H. Vreuls, PhD,[f] Paul J. van Diest, PhD,[f] A.M. Gijs van Leeuwen, MD,[g] Joost van Gorp, PhD,[g] Marielle E.P. Philippens, PhD,[a] Bram van Asselen, PhD,[a] Jan J.W. Lagendijk, PhD,[a] Helena M. Verkooijen, PhD,[h,i] H.J.G. Desirée van den Bongard, PhD,[j] and Antonetta C. Houweling, PhD[a]

[a]Department of Radiation Oncology, UMC Utrecht, Utrecht, the Netherlands; [b]Computational Imaging Group for MRI Diagnostics and Therapy, Center for Image Sciences, UMC Utrecht, Utrecht, the Netherlands; [c]Department of Radiology, UMC Utrecht, Utrecht, the Netherlands; [d]Image Sciences Institute, UMC Utrecht, Utrecht, the Netherlands; [e]Department of Radiation Oncology, RadboudUMC, Nijmegen, the Netherlands; [f]Department of Pathology, UMC Utrecht, Utrecht, the Netherlands; [g]Department of Pathology, St Antonius Hospital, Nieuwegein, the Netherlands; [h]Imaging Division, UMC Utrecht, Utrecht, the Netherlands; [i]Utrecht University, Utrecht, the Netherlands; [j]Department of Radiation Oncology, Amsterdam University Medical Centers, Amsterdam, the Netherlands

Received March 9, 2021; accepted November 1, 2021

Abstract

Purpose: We aimed to evaluate changes in dynamic contrast-enhanced (DCE) and diffusion-weighted (DW) magnetic resonance imaging (MRI) scans acquired before and after single-dose ablative neoadjuvant partial breast irradiation (NA-PBI), and explore the relation between semiquantitative MRI parameters and radiologic and pathologic responses.

Methods and Materials: We analyzed 3.0T DCE and DW-MRI of 36 patients with low-risk breast cancer who were treated with single-dose NA-PBI, followed by breast-conserving surgery 6 or 8 months later. MRI was acquired before NA-PBI and 1 week, 2, 4, and 6 months after NA-PBI. Breast radiologists assessed the radiologic response and breast pathologists scored the pathologic response after surgery. Patients were grouped as either pathologic responders or nonresponders (<10% vs ≥10% residual tumor cells). The

Sources of support: This study received funding from Pink Ribbon (2012.WO22.C154). The funders/sponsors had no role in the design and conduct of the study; collection, management, analysis, and interpretation of the data; preparation, review, or approval of the manuscript; and decision to submit the manuscript for publication.

Disclosures: Drs van den Bongard and van Asselen received funding from Pink Ribbon/Koningin Wilhelmina Fonds voor de Nederlandse Kankerbestrijding (2012.WO22.C154).

Research data are not available at this time.

*Corresponding author: Jeanine E. Vasmel, MD; E-mail: j.e.vasmel@umcutrecht.nl

[1] J.E.V. and M.L.G.K. contributed equally to this work.

https://doi.org/10.1016/j.adro.2021.100854

semiquantitative MRI parameters evaluated were time to enhancement (TTE), 1-minute relative enhancement (RE_{1min}), percentage of enhancing voxels (%EV), distribution of washout curve types, and apparent diffusion coefficient (ADC).

Results: In general, the enhancement increased 1 week after NA-PBI (baseline vs 1 week median − TTE: 15s vs 10s; RE_{1min}: 161% vs 197%; %EV: 47% vs 67%) and decreased from 2 months onward (6 months median − TTE: 25s; RE_{1min}: 86%; %EV: 12%). Median ADC increased from 0.83×10^{-3} mm^2/s at baseline to 1.28×10^{-3} mm^2/s at 6 months. TTE, RE_{1min}, and %EV showed the most potential to differentiate between radiologic responses, and TTE, RE_{1min}, and ADC between pathologic responses.

Conclusions: Semiquantitative analyses of DCE and DW-MRI showed changes in relative enhancement and ADC 1 week after NA-PBI, indicating acute inflammation, followed by changes indicating tumor regression from 2 to 6 months after radiation therapy. A relation between the MRI parameters and radiologic and pathologic responses could not be proven in this exploratory study.

Introduction

Recent studies have investigated hypofractionated neoadjuvant partial breast irradiation (NA-PBI) for patients with early stage breast cancer and a low risk of local recurrence, aiming to reduce overall treatment time and irradiated volume, and thus treatment-related toxicity.[1,2] In a recent trial on single-dose ablative NA-PBI including 36 patients with low-risk breast cancer at our department, 15 patients (42%) showed a pathologic complete response (pCR) and 12 patients (33%) a near pCR. Surgery might be redundant in patients achieving pCR or near pCR after NA-PBI. To accomplish omission of surgery, pathologic response needs to be adequately predicted. In our trial, 10 of 15 patients with pCR, but also 5 of 21 patients without pCR, showed a radiologic complete response on magnetic resonance imaging (MRI) just before breast-conserving surgery (BCS), which resulted in a positive predictive value (ie, probability that radiologic complete response on MRI predicts pCR) of 67% and a negative predictive value (ie, probability that no radiologic complete response on MRI predicts residual disease) of 76%.[3] Therefore, the qualitative clinical response assessment on MRI was insufficient to predict pathologic response in patients after NA-PBI.

Studies on patients with breast cancer treated with neoadjuvant chemotherapy have shown that pathologic response could be predicted using a (semi)quantitative analysis of MRI, although not in patients with low-risk breast cancer.[4–7] Recently, 2 studies reporting on response assessment after high-dose NA-PBI showed significant changes in quantitative MRI parameters acquired before and 1 to 3 weeks after NA-PBI, but these results were not correlated to pathologic response.[8,9] Mouawad et al. reported a significant change in the kinetic parameter K^{trans} calculated from dynamic contrast-enhanced (DCE)-MRI.[9] Wang et al. reported a dependency between radiation dose and direction of apparent diffusion coefficient (ADC) change calculated from diffusion-weighted (DW)-MRI in a subgroup analysis.[8]

The aim of our study was to evaluate changes in MRI up to 6 months after single-dose ablative NA-PBI, and explore a potential relationship between MRI parameters and both radiologic and pathologic responses.

Methods and materials

Study population and treatment

The study population consisted of 36 women with low-risk breast cancer participating in a single-arm, prospective, interventional study at the Department of Radiotherapy of the University Medical Center Utrecht (ClinicalTrials.gov identifier: NCT02316561).[3,10] The institutional review board approved the trial, and all patients gave written informed consent for inclusion. The median age was 65 years (range, 51-78 years), and the median largest tumor diameter at baseline MRI was 13 mm (range, 5-20 mm). All patients had an estrogen receptor-positive and human epidermal growth factor receptor 2-negative tumor.

Patients were treated with a single-dose ablative NA-PBI of 20 Gy to the planning target volume (PTV) of the gross tumor volume (GTV) and 15 Gy to the PTV of the clinical target volume (CTV; CTV = GTV + 2 cm), with a 3 mm PTV margin for both GTV and CTV (Figure E1). A diagnostic biopsy marker was used for position verification. If no marker had been placed during the biopsy or if it was not visible on cone beam computed tomography scanning, a gold fiducial marker (Visicoil, IBA Dosimetry, Germany) was placed. Patients underwent BCS 6 months (n = 15) or, after a study protocol alteration, 8 months (n = 21) after radiation therapy. Six patients (17%) received additional neoadjuvant endocrine treatment after NA-PBI according to national guidelines.[11]

Magnetic resonance imaging acquisition

Patients underwent 3.0T MRI (Ingenia, Philips, the Netherlands) in the prone position using a dedicated 16-channel breast coil before radiation therapy (baseline) and after radiation therapy at 1 week, 2, 4, 6, and, if

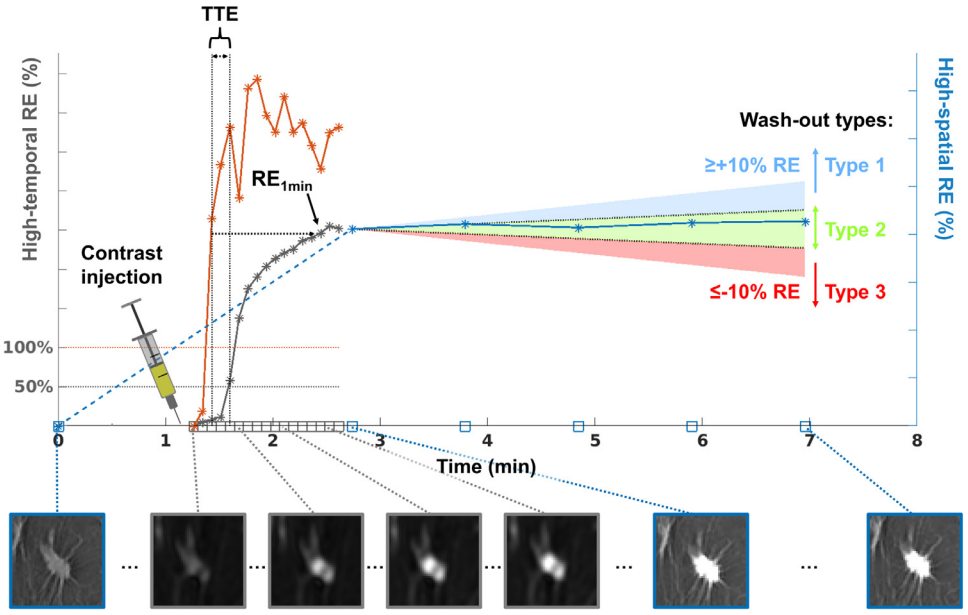

Fig. 1 High-temporal (gray boxes) and high-spatial (blue boxes) dynamic contrast-enhanced-magnetic resonance imaging acquisition showing: median relative enhancement (RE) in aorta region of interest (orange) and 90th percentile RE in gross tumor volume-region of interest in the high-temporal (gray) and high-spatial dynamic contrast-enhanced (blue) series. The vertical dashed lines indicate the onset of aorta enhancement (left) and gross tumor volume enhancement (right). Indicated semiquantitative parameters are time to enhancement (TTE), 1-minute relative enhancement (RE_{1min}), and cutoff boundaries (−10% and +10% RE) for voxel-wise washout curve type classification.

applicable, 8 months. The scan protocol included a DW-MRI series, a high-temporal/low-spatial resolution 3-dimensional T1-weighted DCE-MRI series (referred to as high-temporal) and a low-temporal/high-spatial resolution 3-dimensional T1-weighted DCE-MRI series (referred to as high-spatial). Scan parameters are presented in Appendix B. The DW-MRI (b-values 0; 150 and 800 s/mm^2) was acquired before contrast injection using single-shot echo planar imaging. ADC maps were reconstructed by a monoexponential fit using the scanner's software. The high-temporal DCE-MRI series consisted of 17 rapid full 3-dimensional volumes acquired during the first 90 seconds after contrast injection (Gadovist, Bayer; injection 0.1 mL/kg at 1 mL/s). The high-spatial DCE-MRI series consisted of 6 full 3-dimensional volumes, with the first acquired before contrast injection and the remaining 5 acquired in the 5 minutes directly after the high-temporal DCE series (Fig. 1). Both DCE series were acquired using a T1-weighted, fast-field, echo sequence (spoiled gradient echo). All sequences were acquired with spectral attenuated inversion recovery fat suppression.

Clinical response assessment

Expert breast radiologists qualitatively assessed radiologic response at each scan moment after NA-PBI according to clinical practice in neoadjuvant systemic treatment, and were blinded to the pathologic response. The MRI scans were scored as radiologic complete response, defined as the absence of pathologic contrast enhancement and absence of diffusion restriction, or no radiologic complete response. A radiologic complete response was seen in 1 patient (3%) at 1 week, 6 patients (17%) at 2 months, 9 patients (26%) at 4 months, and 14 patients (40%) at 6 months after NA-PBI.[3]

The pathologic response was evaluated on the surgical specimen and classified as pCR (no residual tumor cells), near pCR (<10% residual tumor cells), partial response (10%-50% residual tumor cells), stable disease (>50% residual tumor cells), or no evidence of response according to the European Society of Breast Cancer Specialists criteria.[12] Fifteen of 36 patients (42%) showed pCR, 12 patients (33%) near pCR, 7 patients (19%) a partial response, and 2 patients (6%) stable disease, but none of the patients had no evidence of response.[3] Patients were grouped as either responders (pCR and near pCR) or nonresponders (all other patients) for further analysis.

Semiquantitative response assessment

Tumor delineation and image registration

Two researchers delineated the GTV on the first postcontrast image of the high-spatial DCE baseline MRI (ie, before NA-PBI) under supervision of a breast radiation oncologist and breast radiologist. To

determine the onset of contrast wash-in in the aorta, a fixed region of interest (ROI) was placed in the descending aorta (aorta-ROI) in the high-temporal DCE-MRI at each scan moment.

Rigid registrations were applied to transform the GTV delineation from the baseline MRI to the MRI acquired after NA-PBI (Fig. 2) and correct for motion between and within both DCE series.[13] To correct for geometric distortions in the DW series, we performed a deformable registration using a B-spline transform to register the DW series to the high-spatial DCE series.[13,14] After the registrations, the final GTV-ROIs for the semiquantitative analysis were created by expanding the transferred GTV delineations with a 1-voxel margin to account for delineation and registration inaccuracies.

MRI scans and registrations were visually assessed. MRI scans affected by artefacts (eg, failure of fat suppression, distortion in GTV region caused by marker) and MRI scans to which the GTV delineation could not be correctly transferred were excluded from analysis, as well as DW series that could not be registered correctly to the DCE series.

Semiquantitative analysis

At each scan moment we computed the following parameters for the GTV-ROI (Fig. 1): in the high-temporal DCE series: 1) time to enhancement (TTE) and 2) 1-minute relative enhancement (RE_{1min}). TTE is the time difference between contrast reaching the aorta and the tumor,[15,16]

$$TTE = t_{tumor} - t_{aorta}$$

where t_{aorta} is the first timepoint with ≥100% increase in median relative enhancement (RE) within the aorta-ROI and t_{tumor} the first timepoint with ≥50% increase in the 90th percentile RE within the GTV-ROI. If the t_{tumor}-threshold was not reached, t_{tumor} was set to the time of the last high-temporal DCE image plus an additional 5 seconds. RE_{1min} is the 90th percentile RE value in the GTV-ROI at 1 minute after enhancement of the aorta.[30,32]

In the high-spatial DCE series: 3) percentage of enhancing voxels (%EV) and 4) relative distribution of washout curve types for enhancing voxels. %EV is the percentage of voxels in the GTV-ROI with >100% RE at the first

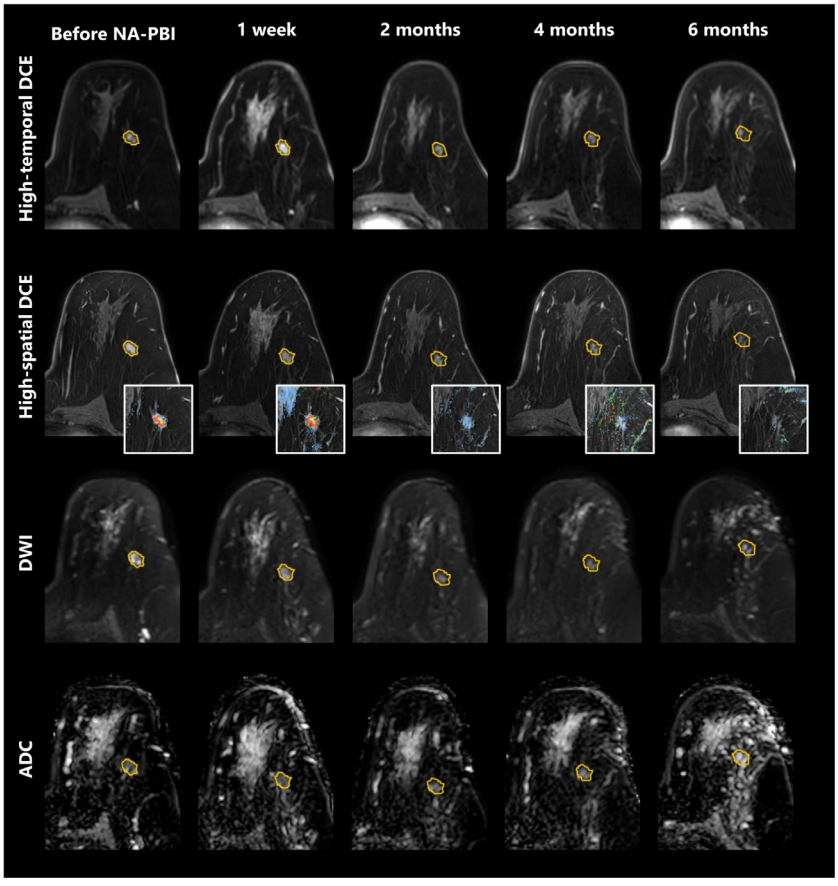

Fig. 2 Overview of all magnetic resonance images acquired in a single patient and gross tumor volume-regions of interest used for analysis (yellow). The high-spatial dynamic contrast-enhanced magnetic resonance imaging (MRI) insets show the washout curve types for the voxels >100% relative enhancement: Type 1 (blue), type 2 (green), and type 3 (red). This patient had no radiologic complete response at any moment and showed a near pathologic complete response (<10% residual tumor cells) after surgery.

postcontrast image.[18,19] Relative distribution of washout curve types for enhancing voxels is determined from the voxel-wise RE difference between the first and last postcontrast injection images, and defined as type 1 (≥+10% RE) −low probability of malignancy, type 2 (−10% to +10% RE) −intermediate probability of malignancy, and type 3 (≤−10% RE)−high probability of malignancy.[4,20,21]

In the DW series: 5) median ADC value.

For both DCE series, the RE was determined as:

$$RE(t) = \frac{SI(t) - SI(0)}{SI(0)} \times 100\%$$

where SI is the signal intensity, t = 0 the precontrast injection image, and t > 0 the postcontrast injection images. In the high-spatial DCE series, a Gaussian filter (3 × 3 × 3 voxels; 0.5 standard deviation) was applied to reduce influence of noise. All semiquantitative analyses were performed using Matlab.[17]

Statistical analysis

Semiquantitative parameters were analyzed using descriptive statistics (median and interquartile range [IQR]) for the entire cohort, by qualitative radiologic response group, and by pathologic response group, using Rstudio, version 1.1.453.[22] No further statistical tests were performed due to the small number of included patients. We analyzed MRI scans obtained up to 6 months after NA-PBI for all 36 patients. The analyses of the 8 months MRI scans of the 21 patients who underwent surgery at 8 months after NA-PBI are presented in Appendix C.

Results

We analyzed 163 high-temporal and 161 high-spatial DCE series and 115 DW series out of a total of 180 scans. Five high-temporal DCE series, 7 high-spatial DCE series, and 5 DW series were not or incorrectly acquired (ie, no precontrast image available, interrupted before end of dynamic series, or incorrectly saved). We excluded the high-temporal and high-spatial DCE series of 12 scan moments in 10 patients from the analysis because the registration of the delineation could not be performed (n = 9) or because fat suppression had failed (n = 3). We excluded all DW series of 8 patients because the DW series could not be correctly registered to the DCE-MRI. The DW series of 20 scan moments in 14 additional patients were excluded because registration could not be performed (n = 17) or fat suppression had failed (n = 3).

The median volume for the analysis was 1.17 mL (IQR, 0.57-1.78) for the high-spatial DCE series, 1.57 mL (IQR, 0.86-2.28) for the high-temporal DCE series, and 1.40 mL (IQR, 0.72-1.80) for the ADC-analyses.

Table 1 Median (IQR) semiquantitative parameter values before and after neoadjuvant partial breast irradiation for the full patient population

Parameter	Baselinemedian (IQR) [n]	1 wk median (IQR) [n]	2 mo median (IQR) [n]	4 mo median (IQR) [n]	6 mo median (IQR) [n]
High-temporal DCE series					
TTE (s)	15 (10-18) [35]	10 (10-15) [31]	20 (15-27) [32]	20 (15-30) [34]	25 (18-46) [31]
RE_{1min} (%)	161 (131-202) [35]	197 (143-232) [31]	113 (92-150) [32]	108 (73-160) [34]	86 (57-135) [31]
High-spatial DCE series					
%EV	47 (35-60) [34]	67 (48-82) [30]	30 (9-38) [33]	19 (11-28) [33]	12 (5-20) [31]
%-$washout_{type1}$	22 (15-28) [34]	36 (23-45) [30]	26 (9-33) [33]	15 (9-21) [33]	9 (4-14) [31]
%-$washout_{type2}$	11 (8-14) [34]	11 (4-18) [30]	3 (1-5) [33]	2 (1-4) [33]	1 (1-3) [31]
%-$washout_{type3}$	8 (4-16) [34]	6 (1-21) [30]	1 (0-2) [33]	1 (0-2) [33]	0 (0-2) [31]
DW series					
Median ADC ($\times 10^{-3}$ mm^2/s)	0.83 (0.81-1.08) [26]	1.15 (0.96-1.30) [24]	1.23 (1.00-1.31) [21]	1.22 (0.97-1.54) [24]	1.27 (1.01-1.49) [20]

Abbreviations: %EV = percentage of enhancing voxels; %-$washout_{typex}$ = percentage of voxels with wash-out type curve x; ADC = apparent diffusion coefficient; DCE = dynamic contrast-enhanced; DW = diffusion-weighted; IQR = interquartile range; RE_{1min} = relative enhancement 1-minute after aorta enhancement; TTE = time-to-enhancement
The number of assessable scans per time point is presented [in brackets].

All patients

Semiquantitative parameter values calculated from MRI scans for the entire cohort are shown in Table 1. Median TTE decreased from 15 seconds at baseline to 10 seconds at 1 week after NA-PBI, and increased to 25 seconds at later scan moments. Median RE_{1min} showed an increase from 161% at baseline to 197% at 1 week after NA-PBI, followed by a decrease to 86% at 6 months after NA-PBI. The same pattern was observed for median %EV (47% at baseline, 67% at 1 week, 12% at 6 months) and for $washout_{type1}$ (22% at baseline, 36% at 1 week, 9% at 6 months). A decrease was observed in median $washout_{type2}$ (11% to 1%) and median $washout_{type3}$ (8% to 0%) from baseline to 6 months after radiation therapy. ADC steadily increased from 0.83×10^{-3} mm^2/s at baseline to 1.27×10^{-3} mm^2/s at 6 months after radiation therapy.

Grouped by qualitative radiologic response

Analyses of semiquantitative parameters in relation to radiologists' clinical assessments are depicted in Table 2. Parameters standing out when grouped by qualitative radiologic response are TTE, RE_{1min}, and %EV (Fig. 3). Median TTE increased from 15 seconds (baseline) to 56 seconds in radiologic complete responders versus 20 seconds in radiologic noncomplete responders (6 months). Median RE_{1min} decreased from 161% (baseline) to 54% for radiologic complete responders versus 113% for radiologic noncomplete responders (6 months). Median %EV changed from 46% (baseline) to 5% for radiologic complete responders versus 17% for radiologic noncomplete responders (6 months). Median ADC value changed from 0.83×10^{-3} mm^2/s (baseline) to 1.13×10^{-3} mm^2/s for radiologic complete responders and 1.27×10^{-3} mm^2/s for radiologic noncomplete responders (6 months).

Grouped by pathologic response

Analyses of semiquantitative parameters in relation to pathologic response are depicted in Table 3. The most notable parameters when grouped by pathologic response were TTE, RE_{1min} at 6 months, and ADC value at 4 and 6 months (Fig. 4). Median TTE changed from 15 seconds (baseline) to 25 seconds (6 months) for pathologic responders and from 10 seconds (baseline) to 18 seconds (6 months) for pathologic nonresponders. Median RE_{1min} showed a decrease from 162% (baseline) to 80% (6 months) for pathologic responders versus 161% (baseline) to 123% (6 months) for pathologic nonresponders. Median ADC value increased from 0.87×10^{-3} mm^2/s (baseline) to 1.29×10^{-3} mm^2/s (6 months) for pathologic responders versus 0.77×10^{-3} mm^2/s (baseline) to 0.95×10^{-3} mm^2/s (6 months) for pathologic nonresponders.

Discussion

In this study, we evaluated the response to single-dose ablative NA-PBI in patients with low-risk breast cancer using semiquantitative analyses of repeated MRI scans acquired before and up to 6 months after radiation therapy. In the entire cohort, semiquantitative analyses at 1 week after radiation therapy showed an increase in %EV, indicating acute inflammation, and analyses at 2 to 6 months after NA-PBI showed a decrease in %EV and voxels with a malignant washout curve, and an increase in ADC values, indicating tumor response. %EV, TTE, and RE_{1min} appeared to correspond to differences between radiologic complete responders and noncomplete responders as qualitatively assessed by breast radiologists. This indicates that semiquantitative DCE parameters may correctly distinguish the qualitative radiologic response, even though radiologists mostly rely on more qualitative assessment to determine response. TTE and RE_{1min} at 6 months after NA-PBI and median ADC value at 4 and 6 months after NA-PBI showed interesting trends for the identification of pathologic response groups. However, differences between the qualitative radiologic response groups and differences between the pathologic response groups were not statistically tested in this small cohort.

The initial increase in relative enhancement observed on MRI acquired at 1 week after radiation therapy was also observed in 2 other studies on single-dose (15-21 Gy) NA-PBI.[8,9] Wang et al. suggested that this early response could be used as a response biomarker, but Mouawad et al. argued that the early response demonstrated too much acute inflammatory effects to assess tumor response and proposed to wait at least 2.5 weeks after radiation therapy before performing MRI. Our results at 1 week after NA-PBI confirmed signs of increased enhancement, which most likely indicate radiation therapy-induced acute inflammation.[23,24] Wang et al. reported no changes in ADC 1 week after radiation therapy in their full group of 15 patients, presumably due to the short time interval between radiation therapy and imaging, although their subgroup analysis showed a relative increase in ADC in the highest dose group (21 Gy). Our results showed a similar increase in ADC value 1 week after radiation therapy.

We applied rigid registration for propagation of the GTV delineation between scans acquired at different scan moments. Advantages of this approach are that this ensured the use of the same GTV-ROI for analyses at

Table 2 Median (IQR) semiquantitative parameter values before and after neoadjuvant partial breast irradiation, grouped by radiologic response

Parameter	Radiologic complete response	Baseline median (IQR) [n]	1 wk median (IQR) [n]	2 mo median (IQR) [n]	4 mo median (IQR) [n]	6 mo median (IQR) [n]
High-temporal DCE series						
TTE (s)	Yes	— [0]	20 (20-20) [1]	63 (51-68) [4]	46 (35-66) [9]	56 (46-61) [13]
	No	15 (10-18) [35]	10 (10-15) [30]	15 (14-22) [28]	20 (15-25) [24]	20 (15-20) [18]
RE_{1min} (%)	Yes	— [0]	244 (244-244) [1]	42 (34-60) [4]	53 (45-64) [9]	54 (45-62) [13]
	No	161 (131-202) [35]	194 (139-228) [30]	118 (102-154) [28]	115 (103-164) [24]	113 (89-139) [18]
High-spatial DCE series						
%EV	Yes	— [0]	54 (54-54) [1]	5 (3-12) [4]	10 (7-14) [8]	5 (4-12) [13]
	No	47 (35-60) [34]	68 (46-82) [29]	31 (22-40) [29]	23 (17-30) [24]	17 (11-24) [18]
%-$washout_{type1}$	Yes	— [0]	35 (35-35) [1]	3 (3-10) [4]	7 (5-9) [8]	4 (3-8) [13]
	No	22 (15-28) [34]	38 (23-45) [29]	27 (10-34) [29]	18 (13-24) [24]	11 (9-20) [18]
%-$washout_{type2}$	Yes	— [0]	13 (13-13) [1]	0 (0-0) [4]	1 (1-2) [8]	1 (1-1) [13]
	No	11 (8-14) [34]	11 (4-18) [29]	3 (1-5) [29]	3 (2-5) [24]	3 (1-5) [18]
%-$washout_{type3}$	Yes	— [0]	6 (6-6) [1]	0 (0-1) [4]	1 (0-2) [8]	0 (0-1) [13]
	No	8 (4-16) [34]	7 (1-21) [29]	1 (0-2) [29]	1 (0-2) [24]	1 (0-2) [18]
DW series						
Median ADC ($\times 10^{-3}$ mm^2/s)	Yes	— [0]	— [0]	1.24 (1.13-1.45) [3]	1.25 (0.91-1.70) [5]	1.13 (0.95-1.49) [9]
	No	0.83 (0.80-1.08) [26]	1.15 (0.96-1.30) [24]	1.16 (1.00-1.31) [18]	1.22 (1.00-1.50) [18]	1.27 (1.14-1.44) [11]

Abbreviations: %EV = percentage of enhancing voxels; %-$washout_{typex}$ = percentage of voxels with wash-out type curve x; ADC = apparent diffusion coefficient; DCE = dynamic contrast-enhanced; DW = diffusion-weighted; IQR = interquartile range; RE_{1min} = relative enhancement 1-minute after aorta enhancement; TTE = time-to-enhancement
The number of assessable scans per time point is presented [in brackets].

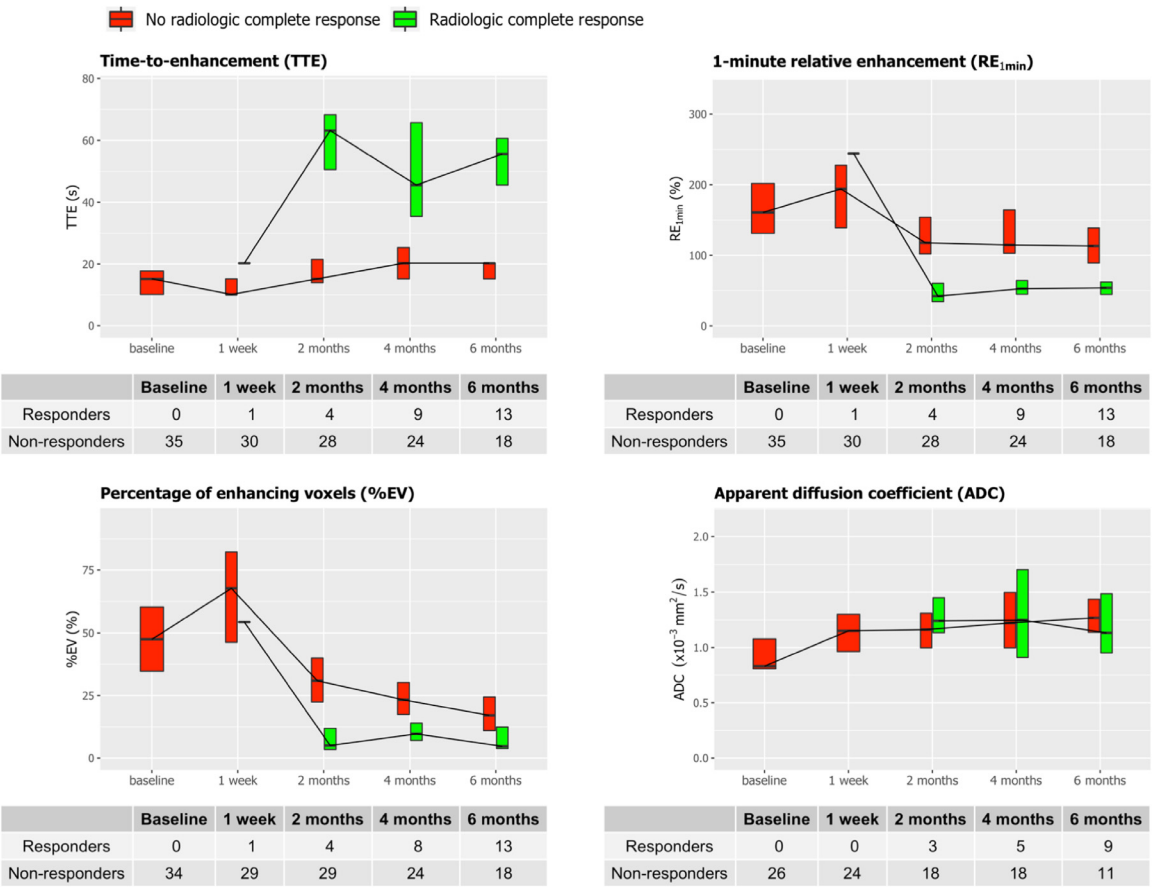

	Baseline	1 week	2 months	4 months	6 months
Responders	0	1	4	9	13
Non-responders	35	30	28	24	18

	Baseline	1 week	2 months	4 months	6 months
Responders	0	1	4	9	13
Non-responders	35	30	28	24	18

	Baseline	1 week	2 months	4 months	6 months
Responders	0	1	4	8	13
Non-responders	34	29	29	24	18

	Baseline	1 week	2 months	4 months	6 months
Responders	0	0	3	5	9
Non-responders	26	24	18	18	11

Fig. 3 Median (interquartile range) semiquantitative parameter values before and after neoadjuvant partial breast irradiation, grouped by qualitative radiologic response along with the number of available scans per scan moment.

each scan moment, was not subject to delineation subjectivity or delineation errors, and that even allowed for us to evaluate MRI parameters in radiologic complete responders. Disadvantages of the approach are that we could not evaluate change in tumor volume over time and that it led to surrounding nontumor tissue entering the ROI for tumors that reduced in volume. We argue that, because mainly fatty tissue or healthy glandular breast tissue, this tissue presents different values for the semiquantitative parameters than tumor tissue.

Another approach for GTV-ROI determination could be to manually adapt the GTV delineation at each scan moment or use deformable image registration to do this, which would have allowed for an evaluation of tumor volume change. However, such an approach is less reproducible and prone to delineation errors. Despite the image registrations, we had to exclude a reasonable number of scans. Because these scans belonged to different patients and were distributed over all scan moments after NA-PBI, this has most likely not influenced the interpretation of the results of the semiquantitative parameters.

In all patients, a marker was introduced for tumor localization, which impeded both the DCE and DW-MRI analyses because this marker lacks MRI signal and distorts the homogeneity of the local magnetic field. Because the marker is present at each scan moment and the artefact will appear largely similar between scans moments, changes in parameters will most likely be due to changes in the tumor tissue. In 2 patients, a marker was inserted between the baseline MRI scan and the first MRI scan acquired after NA-PBI; therefore, we delineated the marker artefact and excluded those voxels from the GTV-ROI at each scan moment. Placing a fiducial marker is necessary for clinical radiologic follow up, position verification during radiation therapy, and tumor localization during surgery; thus, we recommend using a marker that causes only small artefacts on MRI, such as a gold fiducial marker or carbon-coated ceramic marker.[25,26]

A limitation is that our study was designed as a feasibility study for single-dose, ablative, NA-PBI, resulting in too small numbers of patients in the pathologic response groups (27 responders vs 9 nonresponders) to statistically test differences in semiquantitative parameters between the

Table 3 Median (IQR) semiquantitative parameter values before and after neoadjuvant partial breast irradiation, grouped by pathologic response

Parameter	Pathologic complete or near complete response	Baseline median (IQR) [n]	1 wk median (IQR) [n]	2 mo median (IQR) [n]	4 mo median (IQR) [n]	6 mo median (IQR) [n]
High-temporal DCE series						
TTE (s)	Yes	15 (10-19) [26]	10 (10-15) [24]	20 (15-48) [23]	25 (15-35) [25]	25 (20-56) [23]
	No	10 (10-15) [9]	10 (10-15) [7]	15 (15-20) [9]	20 (15-20) [9]	18 (15-20) [8]
RE_{1min} (%)	Yes	162 (128-203) [26]	200 (133-238) [24]	105 (62-145) [23]	97 (64-155) [25]	80 (54-104) [23]
	No	161 (138-193) [9]	191 (170-214) [7]	130 (107-178) [9]	124 (110-161) [9]	123 (106-141) [8]
High-spatial DCE series						
%EV	Yes	40 (32-61) [25]	69 (41-83) [23]	27 (7-34) [24]	18 (10-27) [24]	10 (4-15) [23]
	No	54 (49-60) [9]	66 (57-72) [7]	36 (34-48) [9]	26 (15-42) [9]	20 (12-36) [8]
%-$washout_{type1}$	Yes	21 (12-27) [25]	38 (22-49) [23]	19 (4-28) [24]	14 (7-19) [24]	7 (3-11) [23]
	No	24 (22-37) [9]	35 (26-41) [7]	33 (27-39) [9]	18 (14-36) [9]	14 (10-27) [8]
%-$washout_{type2}$	Yes	10 (7-14) [25]	11 (4-15) [23]	3 (1-5) [24]	2 (1-4) [24]	1 (1-2) [23]
	No	11 (10-16) [9]	19 (13-21) [7]	3 (1-9) [9]	3 (1-5) [9]	3 (2-5) [8]
%-$washout_{type3}$	Yes	8 (3-17) [25]	6 (1-21) [23]	1 (0-2) [24]	1 (0-3) [24]	0 (0-1) [23]
	No	8 (6-13) [9]	15 (6-23) [7]	1 (0-2) [9]	1 (0-2) [9]	1 (0-3) [8]
DW series						
Median ADC ($\times 10^{-3}$ mm^2/s	Yes	0.87 (0.82-1.07) [20]	1.16 (0.99-1.31) [18]	1.23 (1.03-1.31) [17]	1.25 (1.11-1.55) [19]	1.29 (1.13-1.52) [17]
	No	0.77 (0.61-1.15) [6]	0.95 (0.80-1.21) [6]	1.04 (0.76-1.47) [4]	0.99 (0.84-1.01) [5]	0.95 (0.72-1.02) [3]

Abbreviations: %EV = percentage of enhancing voxels; %-$washout_{typex}$ = percentage of voxels with wash-out type curve x; ADC = apparent diffusion coefficient; DCE = dynamic contrast-enhanced; DW = diffusion-weighted; IQR = interquartile range; TTE = time-to-enhancement; RE_{1min} = relative enhancement 1-minute after aorta enhancement.
The number of assessable scans per time point is presented [in brackets].

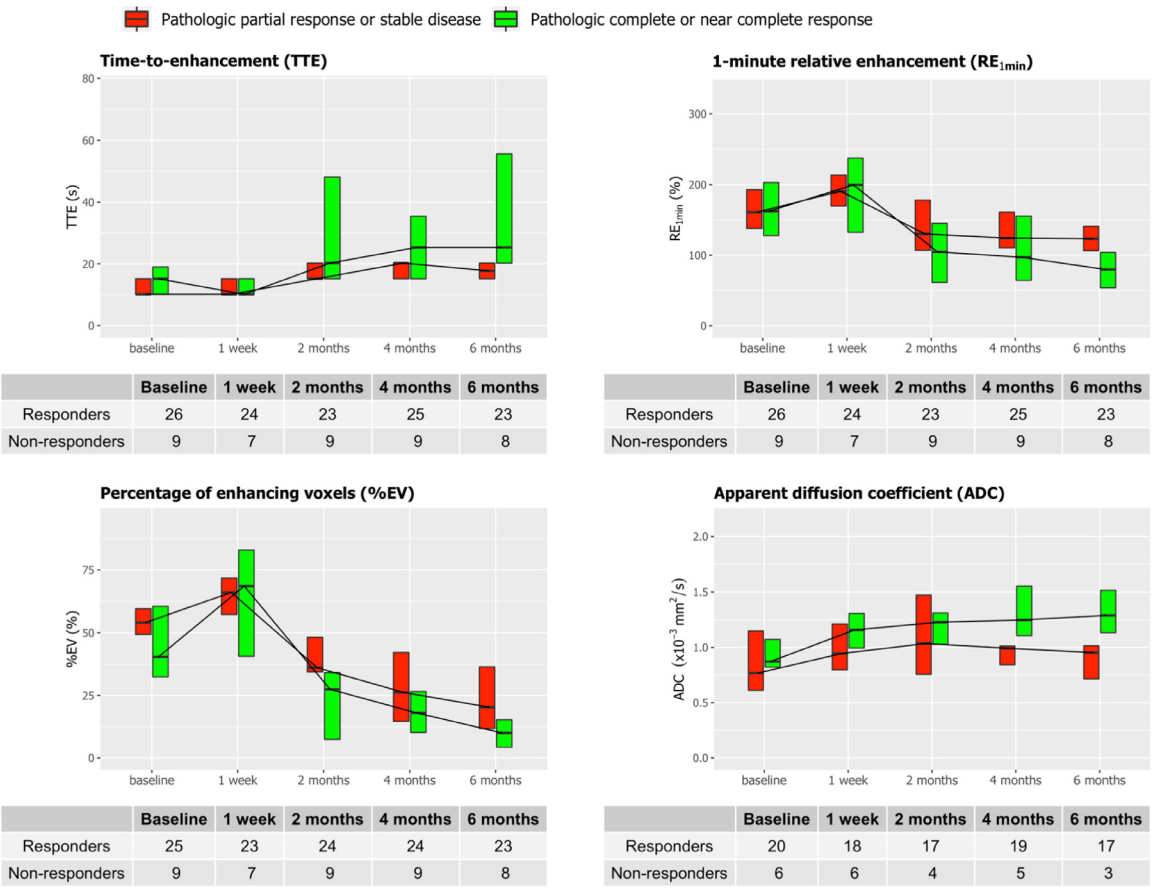

	Baseline	1 week	2 months	4 months	6 months
Responders	26	24	23	25	23
Non-responders	9	7	9	9	8

	Baseline	1 week	2 months	4 months	6 months
Responders	26	24	23	25	23
Non-responders	9	7	9	9	8

	Baseline	1 week	2 months	4 months	6 months
Responders	25	23	24	24	23
Non-responders	9	7	9	9	8

	Baseline	1 week	2 months	4 months	6 months
Responders	20	18	17	19	17
Non-responders	6	6	4	5	3

Fig. 4 Median (interquartile range) semiquantitative parameter values before and after neoadjuvant partial breast irradiation, grouped by pathologic response along with the number of available scans per scan moment.

groups. Although resulting in unevenly sized subgroups, we classified patients with a near pCR as responders because differences between pCR and near pCR cannot be macroscopically distinguished in MRI scans. Furthermore, omitting surgery in patients with near pCR might be safe as well. Another limitation is that our MRI protocol did not include a B0 map to assess and correct distortions and marker artefacts and a T1 map to evaluate quantitative DCE parameters, such as K^{trans} and v_e[27–29]. Semiquantitative analysis of signal-intensity time curves has been shown to correlate well with quantitative assessments.[30,29,31] Therefore, we argue that our semiquantitative approach using available clinical scans is valid.

Ideally, pathologic response can be predicted from MRI acquired before or after NA-PBI to select patients with an excellent pathologic response. In those patients, surgery could be omitted after NA-PBI. We believe that TTE and RE_{1min} at 6 months after NA-PBI and ADC at least 4 months after NA-PBI might contribute to this goal. All other parameters, as well as TTE, RE_{1min}, and ADC at earlier scan moments after NA-PBI, did not indicate differences between the pathologic response groups. This can be valuable information for future studies, and has to be tested in larger cohorts.

Conclusion

The evaluation of semiquantitative parameters derived from DCE-MRI and DW-MRI before and after single-dose ablative NA-PBI showed changes indicating acute inflammation shortly after radiation therapy, followed by changes indicating tumor response up to 6 months after radiation therapy. A clear relation between the MRI parameters and radiologic and pathologic responses could not be proven in this exploratory study. TTE, $RE1_{min}$, and %EV showed the largest differences between radiologic complete and non-complete responders as assessed according to clinical practice. TTE, RE_{1min}, and ADC value at 6 months after NA-PBI are the most promising for differentiation between pathologic responders and nonresponders.

Acknowledgments

The authors thank A. J. Witkamp, R. Koelemij, A. Doeksen, T. van Dalen, M. F. Sier, E. van der Wall, K. G. A. Gilhuijs, J. P. Wijnen, and A. L. H. M. W. van Lier for their contributions to this work.

Supplementary materials

Supplementary material associated with this article can be found, in the online version, at doi:10.1016/j.adro.2021.100854.

References

1. Horton JK, Blitzblau RC, Yoo S, et al. Preoperative single-fraction partial breast radiation therapy: A novel phase 1, dose-escalation protocol with radiation response biomarkers. *Int J Radiat Oncol Biol Phys*. 2015;92:846–855.
2. Van Der Leij F, Bosma SCJ, Van De Vijver MJ, et al. First results of the preoperative accelerated partial breast irradiation (PAPBI) trial. *Radiother Oncol*. 2015;114:322–327.
3. Vasmel JE, Charaghvandi RK, Houweling AC, et al. Tumor response following neoadjuvant MR-guided single ablative dose partial breast irradiation. *Int J Radiat Oncol*. 2020;106:821–829.
4. Abramson RG, Li X, Hoyt TL, et al. Early assessment of breast cancer response to neoadjuvant chemotherapy by semi-quantitative analysis of high-temporal resolution DCE-MRI: Preliminary results. *Magn Reson Imaging*. 2013;31:1457–1464.
5. Galbán CJ, Ma B, Malyarenko D, et al. Multi-site clinical evaluation of DW-MRI as a treatment response metric for breast cancer patients undergoing neoadjuvant chemotherapy. *PLoS One*. 2015;10:e0122151.
6. Tudorica A, Oh KY, Chui SYC, et al. Early prediction and evaluation of breast cancer response to neoadjuvant chemotherapy using quantitative DCE-MRI. *Transl Oncol*. 2016;9:8–17.
7. Dietzel M, Kaiser C, Pinker K, et al. Automated semi-quantitative analysis of breast MRI: Potential imaging biomarker for the prediction of tissue response to neoadjuvant chemotherapy. *Breast Care*. 2017;12:231–236.
8. Wang C, Horton JK, Yin FF, Chang Z. Assessment of treatment response with diffusion-weighted MRI and dynamic contrast-enhanced MRI in patients with early-stage breast cancer treated with single-sose preoperative radiotherapy: Initial results. *Technol Cancer Res Treat*. 2016;15:651–660.
9. Mouawad M, Biernaski H, Brackstone M, et al. DCE-MRI assessment of response to neoadjuvant SABR in early stage breast cancer: Comparisons of single versus three fraction schemes and two different imaging time delays post-SABR. *Clin Transl Radiat Oncol*. 2020;21:25–31.
10. Charaghvandi RK, van Asselen B, Philippens MEP, et al. Redefining radiotherapy for early-stage breast cancer with single dose ablative treatment: a study protocol. *BMC Cancer*. 2017;17:181.
11. Oncoline. Breast cancer guidelines: Dutch guidelines, version 2.0. Available at: https://www.oncoline.nl/index.php?pagina=/richtlijn/item/pagina.php&id=41230&richtlijn_id=1069. Accessed December 17, 2020.
12. European Commission Directorate-General for Health and Consumers (European Commission). In: von Karsa L, Holland R, Broeders M, de Wolf C, Perry N, Törnberg S, eds. *European guidelines for quality assurance in breast cancer screening and diagnosis. Fourth edition, Supplements*. Luxembourg: Office for Official Publications of the European Union; 2013.
13. Klein S, Staring M, Murphy K, Viergever MA, Pluim JPW. Elastix: A toolbox for intensity-based medical image registration. *IEEE Trans Med Imaging*. 2010;29:196–205.
14. Takatsu Y, Sagawa H, Nakamura M, Suzuki Y, Miyati T. Novel distortion correction method for diffusion-weighted imaging based on non-rigid image registration between low b value image and anatomical image. *Magn Reson Imaging*. 2019;57:277–284.
15. Boetes C, Barentsz JO, Mus RD, et al. MR characterization of suspicious breast lesions with a gadolinium- enhanced TurboFLASH subtraction technique. *Radiology*. 1994;193:777–781.
16. Mus RD, Borelli C, Bult P, et al. Time to enhancement derived from ultrafast breast MRI as a novel parameter to discriminate benign from malignant breast lesions. *Eur J Radiol*. 2017;89:90–96.
17. The MathWorks, Inc. MATLAB, version R2019a. Available at: https://mathworks.com/. Accessed February 24, 2020.
18. DeMartini WB, Lehman CD, Peacock S, Russell MT. Computer-aided detection applied to breast MRI: Assessment of CAD-generated enhancement and tumor sizes in breast cancers before and after neoadjuvant chemotherapy. *Acad Radiol*. 2005;12:806–814.
19. Henderson SA, Gowdh NM, Purdie CA, et al. Breast cancer: Influence of tumour volume estimation method at MRI on prediction of pathological response to neoadjuvant chemotherapy. *Br J Radiol*. 2018;91: 20180123.
20. Degani H, Gusis V, Weinstein D, Fields S, Strano S. Mapping pathophysiological features of breast tumors by MRI at high spatial resolution. *Nat Med*. 1997;3:780–782.
21. Partridge SC, Stone KM, Strigel RM, DeMartini WB, Peacock S, Lehman CD. Breast DCE-MRI. *Acad Radiol*. 2014;21:1195–1203.
22. RStudio Team. RStudio: Integrated development for R. Available at: http://www.rstudio.com/. Accessed June 26, 2020.
23. Janssen MHM, Aerts HJWL, Kierkels RGJ, et al. Tumor perfusion increases during hypofractionated short-course radiotherapy in rectal cancer: Sequential perfusion-CT findings. *Radiother Oncol*. 2010;94:156–160.
24. Sawyer B, Pun E, Samuel M, et al. CT perfusion imaging in response assessment of pulmonary metastases undergoing stereotactic ablative radiotherapy. *J Med Imaging Radiat Oncol*. 2015;59:207–215.
25. Chan MF, Cohen GN, Deasy JO. Qualitative Evaluation of Fiducial Markers for Radiotherapy Imaging. *Technol Cancer Res Treat*. 2015;14:298–304.
26. Ghate SV, Baker JA, Hawkins AD, Soher BJ. Titanium vs carbon coated ceramic breast tissue marker clips: 3T MR susceptibility artifact and local signal disturbance. *Acad Radiol*. 2011;18:770–773.
27. O'Flynn EAM, DeSouza NM. Functional magnetic resonance: biomarkers of response in breast cancer. *Breast Cancer Res*. 2011;13:204.
28. Wang LC, DeMartini WB, Partridge SC, Peacock S, Lehman CD. MRI-detected suspicious breast lesions: Predictive values of kinetic features measured by computer-aided evaluation. *Am J Roentgenol*. 2009;193:826–831.
29. Wang CH. Review of treatment assessment using DCE-MRI in breast cancer radiation therapy. *World J Methodol*. 2014;4:46.
30. Jackson A, Li KL, Zhu X. Semi-quantitative parameter analysis of DCE-MRI revisited: Monte-Carlo simulation, clinical comparisons, and clinical validation of measurement errors in patients with type 2 neurofibromatosis. *PLoS One*. 2014;9:e90300.
31. Hayes C, Padhani AR, Leach MO. Assessing changes in tumour vascular function using dynamic contrast-enhanced magnetic resonance imaging. *NMR Biomed*. 2002;15:154–163.
32. Mori N, Pineda FD, Tsuchiya K, et al. Fast temporal resolution dynamic contrast-enhanced MRI: Histogram analysis versus visual analysis for differentiating benign and malignant breast lesions. *Am J Roentgenol*. 2018;211:933–939.